AIAA 80-0240R

Orbit Determination and Prediction Methods for Satellite-Aided Search and Rescue

W.B. Graham* and F.R. Vigneron†
Communications Research Centre, Ottawa, Canada

Methods of obtaining a suitable satellite ephemeris for local user terminals of the satellite-aided search and rescue system are identified. The performances of two methods in which local corrections of orbital position is undertaken are compared. One method involves a least-squares estimator which adjusts the time of epoch plus Doppler bias and the other utilizes a six orbit-state plus Doppler bias Kalman estimator. The epoch-time estimator demonstrates worthwhile properties such as speed of operation and simplicity but reveals a clear dependence upon the error characteristics of the externally-supplied orbital state updates (orbit determinations). This study shows that the mission accuracy requirement of 1 km in orbit position cannot be met by this means although a 3 km orbit-position error is feasible for a mission life of several years. In comparison, the Kalman estimator displays no evidence of a dependence on the orbital state updates and exhibits an accuracy in orbit position of about 0.5 km. Its performance has been demonstrated by using tracking data from LANDSAT III and offers potential for long term independent use.

Introduction

THE objective of the satellite-aided search and rescue mission (SARSAT) is to augment the capabilities of existing search and rescue (SAR) forces to detect and locate emergency locator transmitters (ELT) and emergency position indicating radio beacons (EPIRB).[1] The SARSAT system consists of a space segment with SAR instrument packages to be included onboard the TIROS-N series of spacecraft, NOAA-E, NOAA-F and NOAA-G, and an Earth segment comprising local user terminals (LUTs) and mission control centers (MCC) (one MCC in each of U.S.A., France, and Canada). ELT and EPIRB signals will be received by the satellite SAR instrument and normally will be relayed in real time via a downlink carrier to available LUTs. On acquisition of the spacecraft downlink signal, the LUT will detect and measure the frequency of the retransmitted ELT and EPIRB signals during the satellite pass. The geographic locations of the ELTs and EPIRBs will be computed at the LUTs from the measured Doppler frequency and satellite position, and the information will be conveyed to the appropriate rescue coordination center (RCC) via the MCC.

The satellites will be in nearly polar, circular orbits at an altitude of approximately 850 km. Because of the rapid motion of the spacecraft with respect to the Earth's surface, signals from ELTs, EPIRBs, and the spacecraft generate a well-defined Doppler signature. Calculation of the position of an ELT or EPIRB utilizes the Doppler-shifted frequency measurements as received by the spacecraft SAR instrument, and the orbital position (ephemeris) of the satellite. Errors in the ephemeris contribute a significant part of the error in the estimation of latitude and longitude of the distress site. Thus, a good knowledge of the ephemeris is indispensable for good system performance.[2,3]

The satellite's position must be known to an accuracy of 1.0 km at all times during a pass, in order that this error will be an acceptably small part of the overall error budget. No error limit is prescribed for velocity.

There are a number of ways to obtain the ephemeris at the LUT. This paper discusses the options available and describes two methods in detail that were considered suitable for application in this project.

Presented as Paper 80-0240 at the AIAA 18th Aerospace Sciences Meeting, Pasadena, Calif., Jan. 14-16, 1980; submitted Jan. 18, 1980; revision received Aug. 4, 1980.

*Research Engineer.
†Research Scientist. Member AIAA.

Options for Orbit Determination and Ephemeris Calculation

A first option is to provide an externally-generated ephemeris to each LUT along with an appropriate interpolation scheme.[4] Currently, for the TIROS satellites, NORAD supplies NOAA with a daily orbit determination [(OD) a set of time-tagged orbital state elements]. From this OD, NOAA can predict the satellite position over a five-day period to within 3 km using a sophisticated prediction model.[5] This option requires minimum software at the LUT; however, it has some negative aspects. Expensive high quality transmission lines are required to link the external source with the LUTs. Also, the LUTs cannot operate without the externally-derived data even in a degraded mode. Since LUTs for operational systems may be required to function in remote areas and be unmanned, it is desirable for the LUT to be operable with much less dependence on external data than this option offers.

A second option entails ephemeris generation and epoch time correction at the LUT. In this option, an OD is obtained at regular time intervals and the epoch time of the external OD is adjusted to conform with range-rate data derived from the downlink at the LUT during satellite passes. The ephemeris is calculated using the upgraded OD and an appropriate computer model of the orbit dynamics. The basic assumption involved is that all orbital elements except anomaly can be predicted with sufficient accuracy in the intervals between externally-transmitted updates. The estimator is one which has been utilized successfully elsewhere.[6] It is formulated as a least-squares filter; but, instead of adjusting the six independent epoch states as in a conventional application, the epoch states are held fixed and the time of epoch is adjusted in accordance with the least-squares criterion, hence the reason it is referred to herein as the epoch-time estimator. The stable orbit plane of the TIROS spacecraft makes this an effective scheme even with a very simple orbit-dynamics model. The attraction of this type of estimator is simplicity, efficiency in computation, and low demands on computer core. No specific quantitative analysis or data on performance is available in Ref. 6. In the following sections quantitative analysis of the method is presented.

A third option is an orbit-state estimator-predictor method in which all orbital elements are determined immediately after each satellite pass from downlink-derived range-rate data taken during the pass. Developmental work on an extended Kalman filter orbit estimator has been performed independently from the SARSAT program.[7] Analysis and

performance of this option relative to the SARSAT requirement is discussed.

The second and third options are generically similar in concept, since both derive orbital correction information from the downlink of the SAR instrument. A particular deficiency in the passive measurement of the range rate from the downlink signal is the presence of a bias arising from long term oscillator frequency drift. Since the bias is constant during a pass, it is easily dealt with by estimating its value along with the orbital states of the satellite.

Epoch-Time Estimator

Formulation

Following convention, the differential equations of motion and the observation equation, respectively, are written in the generalized form,

$$\dot{x}=f(x) \tag{1}$$

$$z_k=h(x_k)+v_k \tag{2}$$

where for practical purposes z_k represents the collection of all range-rate observations made during one satellite pass, that is,

$$h_k(x_k)=\{h(x_1),h(x_2),\ldots,h(x_k)\}^T$$

$$v_k=\{v_1,v_2,\ldots,v_k\}^T$$

The vector x contains the orbital position and velocity states and f is the nonlinear vector function representation of the Earth's gravitational potential. The system equations are developed in geocentric Cartesian inertial coordinates.[8] Only forces generated by a uniform oblate Earth are retained in the orbital equations of motion. The observation noise v_k is assumed to be stationary, white, and Gaussian with a zero mean. To facilitate a solution to the estimation problem by means of a least-squares criterion, linearization of Eq. (1) is required. Given a reasonable starting estimate (or OD), $x_0=x(t_0)$, integration of Eq. (2) yields a reference trajectory $\bar{x}(t)$ about which the linearization may be performed; thus,

$$h_k(x_k)\cong h_k(\bar{x}_k)+\left.\frac{\partial h_k(x_k)}{\partial x_k}\right|_{x_k=\bar{x}_k}\delta x_k \tag{3}$$

where $\delta x_k=(x_k-\bar{x}_k)$.

Since a fundamental assumption is that the only significant error is in the prediction of the in-track position, this may be viewed as an error in timing; that is, the satellite's coordinates at epoch may remain unchanged and instead an adjustment of the time tag of epoch may be made to effect an improvement of the estimated orbit state. This is quantified by the expression,

$$\delta x_0\cong f(x_0)\,\delta t_0$$

Thus, the differential correction of the epoch-state coordinates equivalent to the timing correction sought is constrained according to the dynamic equations of motion. Since the adjustment of time of epoch is a translation of the time axis, that is, $\delta t=\delta t_0$, then

$$\delta x\cong f(\bar{x})\,\delta t_0 \tag{4}$$

and using Eq. (1),

$$\delta x_k=\dot{\bar{x}}_k\delta t_0 \tag{5}$$

Substitution of Eq. (5) in Eq. (3) yields

$$h_k(x_k)\cong h_k(\bar{x}_k)+\left.\frac{dh_k(x_k)}{dt_k}\right|_{x_k=\bar{x}_k}\delta t_0 \tag{6}$$

By defining the residual vector

$$\delta z_k=z_k-h_k(\bar{x}_k) \tag{7}$$

the required solution is the least-squares estimate for δt_0 of the system of equations,

$$\delta z_k=H_k\delta t_0 \tag{8}$$

in which

$$H_k=\left.\frac{dh_k(x_k)}{dt}\right|_{x_k=\bar{x}_k}$$

The estimated epoch-time correction is therefore

$$\delta t_0=(H_k^TH_k)^{-1}H_k^T\delta z_k \tag{9}$$

To account for the Doppler-bias constant, its estimation is performed by treating it as a state variable. The state equations are augmented appropriately. Finally, because this estimation algorithm is developed through linearization, iteration upon each solution until convergence is achieved is necessary for best performance.

Performance

Simulated spacecraft orbital data were generated for testing purposes. The data set was produced from a modified version of the Goddard trajectory determination system (GTDS) software package and consists of orbital state vectors, representative of a TIROS-N spacecraft orbit, in inertial Cartesian form spaced at one minute intervals. The dynamics model used for this purpose includes a 15th order and 15th degree (15×15) geopotential gravitational field, lunisolar perturbations, air drag, and solar radiation pressure perturbations. Also, a program was created to evolve from this data simulation of range-rate measurements such as would normally be obtained in an Earth-based receiving station.

Initially, some simple tests were done to obtain insight into the capability of the estimator.[8] Convergence criteria and sampling rates were established provisionally by adopting "perfect" dynamics; that is, the "true" orbit trajectory was generated by a set of equations of motion exactly the same as those of the filter. Tests of this nature were run for one satellite pass. Effective correction ability was maintained by the filter for corrections $\delta t_0>1$ ms and $\delta b>1$ m/s (approximately 7.5 m along track error and 5 Hz Doppler frequency bias). A sampling rate of 10 samples per minute appeared to sustain the estimator accuracy over a fairly wide range of realistic signal bias and noise levels.

Since the estimator is not intended to correct cross-track errors, it is of some importance to ensure reasonable accuracy in prediction of these components. Figure 1 is an illustration of the comparison of the errors on day 7 for three geopotential field descriptions taken with respect to the 15×15 field model. The initial conditions are error free. When only the second zonal harmonic J_2 is included in the predictor dynamics, cross-track errors can contribute several kilometers to the errors and at this point appear to be continuing to grow. Inclusion of the third zonal harmonic J_3 induces a marked reduction in both the altitude error and the oscillation of the in-track error. Inclusion of the fourth zonal harmonic J_4 results in a like reduction of the cross-track error and almost a 40% improvement of the in-track component. Thus, over the period of this seven-day trial the cross-track errors are bounded to within about 0.5 km with J_2, J_3, J_4 included in the dynamics.

A feasibility test of the estimator is exemplified in Fig. 2. A perfect initial condition is assumed. The curve with the discontinuities represents the results with the estimator functioning and the adjacent curve represents the prediction only. Note the significant corrections of the in-track com-

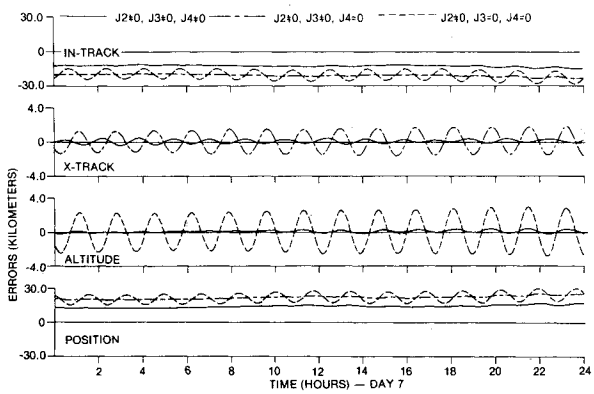

Fig. 1 Errors in prediction model on day 7 for three geopotential field descriptions, error-free initial conditions.

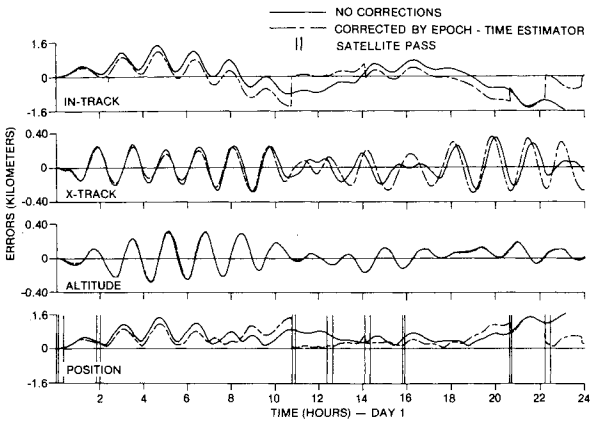

Fig. 2 Performance of epoch-time estimator, error-free initial conditions.

ponent while the effects upon cross-track errors are negligible. The somewhat poor effort by the estimator in response to the data from the pass between 20:00 and 21:00 h can be attributed to the fact that this pass is only slightly over 3 min long; that is, it is a very low elevation-angle pass (which would not normally be considered useful) and the Doppler signature is ill defined.

The ultimate test of the filter was made through a set of Monte Carlo runs. An approximate knowledge of the error characteristics of the ODs is available.[5] It is estimated that the errors are bounded in 1) position <0.4 km, and 2) velocity <50 cm/s. Statistics of the OD errors are not available from the source (NORAD). For the purpose of establishing a hopefully realistic representation of an OD, certain assumptions were made. All components of the OD error were assumed to be independent, Gaussian random variates with zero means and with equal variances in position and velocity coordinate errors respectively, that is,

$$\sigma_x = \sigma_y = \sigma_z = \sigma_p \qquad \sigma_{\dot{x}} = \sigma_{\dot{y}} = \sigma_{\dot{z}} = \sigma_v$$

where

$$3\sigma_p^2 = \sigma_{pm}^2, \qquad 3\sigma_v^2 = \sigma_{vm}^2$$

and

$$3\sigma_{pm} = 0.4 \text{ km} \qquad 3\sigma_{vm} = 50.0 \text{ cm/s}$$

Thus, when an OD was desired (which was assumed every 24 h) a state was extracted from the true data base at the appropriate time and was corrupted in accordance with this approximation. To retain practical dimensions to the studies the data base was restricted to 7 days of data and 12 runs in

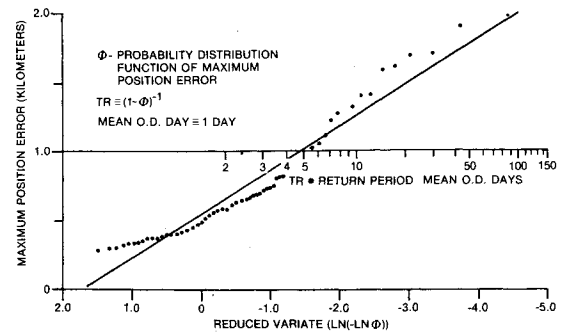

Fig. 3 Performance of epoch-time estimator, without OD rejection/acceptance.

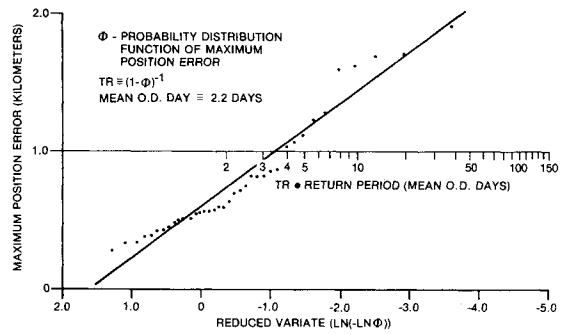

Fig. 4 Performance of epoch-time estimator, with OD rejection/acceptance.

total were made, thus providing 84 OD (daily) events for analysis. Only passes of duration of 10 min or longer were processed by the estimator.

Output from the runs consisted of maximum position magnitude errors for each pass. From this data the maximum values for each day (i.e., OD event) were selected and ordered according to magnitude. Using the order statistics, two one-sided confidence intervals were computed. From the results of these calculations the following statements may be made: 1) the probability is 0.99 that 95% of the daily maximum position-error population is less than 2 km and 2) the probability is 0.99 that 69% of the daily maximum position-error population is less than 1 km. Statement 1 might be considered an overall performance index. Statement 2 relates the estimator performance to the SARSAT error criterion of 1 km. The latter statement indicates that it is probable that about a third of the daily maximum position-error population will be in excess of 1 km.

Further runs were made, that included in the estimator the ability to reject or accept an OD. A simple approach is one which makes a decision based upon the relative magnitudes of the mean value of the squared measurement residuals (MVSMR) obtained from running the estimator (using the observation data from one pass), first with the estimator's current conditions and then with the new OD as a starting condition.[9] In effect, if K*MVSMR ($K \geq 1$, a chosen constant) is greater than the MVSMR using a new OD, the OD is accepted, otherwise it is rejected. For the runs reported here K is unity. In addition, a probability of 0.01 is assigned to the likelihood of not receiving an OD at all. Again a total of 12 runs were conducted. Of the 84 ODs available, 46 were rejected and 1 was not received by the estimator. Thus the estimator performed for an average of 2.2 days between accepted ODs.

As described earlier, a similar selection and ordering process of the output was done. For the purpose of comparing the results of this group of runs with the other, the order statistics of both groups were analyzed according to Gumbel.[10,11] Figures 3 and 4 show the maximum position error vs

the return period (reciprocal of one minus the probability) for the set of runs without OD rejection/acceptance and with OD rejection/acceptance criteria, respectively. Straight-line, least-squares-fit curves are also shown in each case. The respective interpretation of these two graphs relative to the 1 km error criterion may be stated as follows: 1) without OD rejection criteria, on the average the position error will equal or exceed 1 km once in 4.7 days and 2) with OD rejection criteria, on the average the position error will equal or exceed 1 km once in 7.7 days.

These observations make it clear that while protection against gross error may be provided, only marginal improvement in effective performance results from screening the ODs. The rigour of statement 2 may be challenged to some extent since the ODs used to start each of the 12 runs are not subjected to residual tests as would be so in reality; however, because the probability curve is a fitted curve (i.e., a representative average) the effects of these omissions are only very slight.

Generally, the performance of the epoch-time estimation method is dependent on the quality of the external orbit determination. It works well if the orbit determination errors are in-track positional errors (or equivalently, errors in timing), but it cannot respond to velocity errors.

Orbit-State Kalman Estimator/Predictor

Formulation

The estimator utilized is an extended Kalman filter. The derivation of the filter equations is given in many textbooks.[12,13]

The extrapolation equations for time t_{k+1}, given all data up to and including t_k, are

$$\dot{x}_{k+1/k} = f(x_{k+1/k}) \tag{10}$$

for the state estimate, and

$$P_{k+1/k} = \Phi(k+1,k) P_{k/k} \Phi^T(k+1,k) + Q_{k+1} \tag{11}$$

for the error covariance matrix. $\Phi(k+1,k)$ is the state-transition matrix defined by

$$\Phi_{(k+1,k)} = \frac{\partial x_{k+1}}{\partial x_k}$$

and Q_{k+1} is the state-noise covariance matrix. The update equations at time $t_k + 1$ are

$$x_{k+1/k+1} = x_{k+1/k} + K_{k+1}[z_{k+1} - h_{k+1}(x_{k+1/k})] \tag{12}$$

for the state estimate, and

$$P_{k+1/k+1} = \Lambda_{k+1} P_{k+1/k} \Lambda_{k+1}^T + K_{k+1} R_{k+1} K_{k+1}^T \tag{13}$$

for the matrix of error covariances, where

$$\Lambda_{k+1} = I - K_{k+1} H_{k+1}$$

and R_{k+1} is the variance of measurement noise. The Kalman gain is

$$K_{k+1} = P_{k+1/k} H_{k+1}^T (H_{k+1} P_{k+1/k} H_{k+1}^T + R_{k+1})^{-1} \tag{14}$$

The generalized measurement model

$$z = h(x) + v \tag{15}$$

defines the nonlinear measurement function from which the "measurement" matrix

$$H_{k+1} = \frac{\partial h(x)}{\partial x} \Big|_{x = x_{k+1/k}} \tag{16}$$

is established.

The observations enter the algorithm as scalars and therefore the inverse term in the expression for the Kalman gain, Eq. (16), is also a scalar.

The measurement noise R_{k+1} and the state noise matrix Q_{k+1} are used to tune the filter. It is customary to assign R_{k+1} the value of the known measurement noise variance. The major role of the matrix Q_{k+1} in a practical sense is to prevent filter divergence. The choice of Q_{k+1} is one of selecting a suitable matrix that ensures that the propagation of the matrix of error covariances is a reasonable representation of the actual error covariances. A simple choice is to assume Q_k to be diagonal and to extrapolate Q_{k+1} according to

$$Q_{k+1} = Q_k \delta t' \tag{17}$$

where $\delta t'$ is some multiple of a chosen time step. The initial value Q_0 is obtained as a result of performing a sufficient number of tests on the filter to provide acceptable performance.

The Kalman filter of Eqs. (10-19) is a sequential estimator. In the current LUT design, it is treated as a batch processor and is supplied with a set of observations at the end of each satellite pass. Upon completion of the sequential estimation procedure, the final processed estimate is used as an initial state and the filter dynamics then "predicts" a trajectory backwards over the pass; consequently, errors referred to herein refer to errors relative to the final trajectory and do not relate to errors associated with estimator transient behavior.

Of a number of orbital state formulations possible, inertial Cartesian coordinates are used in the estimator because the simpler form of the equations permits slightly better use of computer core.

For orbit prediction by numerical integration the unified state model[14] (USM6) is used with up to fourth-order zonal harmonics in the gravitational field. Earlier independent studies[15] demonstrate that the unified state model is more efficient than other methods from the standpoint of speed and accuracy (for example, for a low Earth satellite in a circular orbit, integration with USM6 can obtain the same accuracy as with inertial Cartesian coordinates but with up to 15 times the integration step size). In these studies and subsequently, the Runge-Kutta Gill fourth-order algorithm was used for all numerical integration.

Performance Characteristics

Two simple runs were done on this filter to demonstrate its ability to satisfy SARSAT requirements readily; one run used a good starting condition that reflected an error in timing only and the other used a starting condition that had a substantial velocity error. In these cases, the true state was based upon a dynamics perturbation model as described previously but with a fourth order and fourth degree description of the geopotential; the filter dynamics included only the second zonal harmonic of the geopotential in order to retain a definite discrepancy with respect to the true dynamics. Over a test period of one day, a satisfactory result was obtained in both runs. Typically, errors in position during passes were less than 400 m while maximum prediction errors in both position and velocity between passes decreased with time, indicating knowledge of the true orbit is improved over that time period.

Tests using simulated data of five days duration have been conducted. The starting condition was assumed to have an error of approximately 500 m in position and about 100 cm/s in velocity, values well over maximum expected OD errors. There is no appreciable difference in the results between these and the initial runs cited previously.

Figure 5 is a sample of the rms position error taken from the second half of the second day. The solid-line curve is the error believed to exist by the estimator (extracted from the error covariance matrix) and the broken-line curve is the actual error. The a priori covariance matrix in this case was

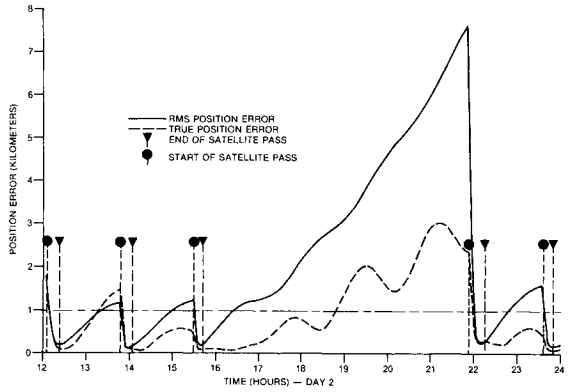

Fig. 5 Example of Kalman estimator performance.

assumed diagonal but reflected in these elements (i.e., the variances) a fairly close representation of the true errors.

Tests with LANDSAT-III Data

An experiment was set up to attempt to track and receive a suitable signal from LANDSAT-III (using CRC Ottawa ground station), a spacecraft which has an orbit closely similar to the TIROS-N spacecraft. This proved impractical. Subsequently, seven days of raw tracking data for this spacecraft were supplied by NASA[16] to allow the proposed test to be undertaken. As a data source for testing the estimator's performance, seven days of definitive orbit data (estimates of the orbit states, within 200 m of true states) covering the same period as the raw tracking data were also supplied by NASA.[17]

A bias was added to the real tracking data (two-way Doppler measurements) to simulate its presence as in the SARSAT system and the range-rate bias was included in the Kalman estimator as an additional state to be estimated. Tracking data in the SARSAT system is to be supplied at a rate of one point every 30 s and this rate of data input was used for the tests.

Eleven runs were performed to tune the filter (i.e., to choose R and Q), which were followed by a final run incorporating these values to demonstrate conclusive estimator design performance.[18] The 10 s averaging time used in the real tracking data tends to diminish the noise characteristics; thus, while errors in the measured data were very small, a measurement noise variance based upon the apparent magnitude of variation proved unrealistically small for the estimator. It was found in fact that a standard deviation of 2 m/s was suitable. Two runs were executed with identical parameters but with measurement models based upon an instantaneous and an approximate 10 s average range rate, respectively. There appeared to be no decisive basis to prefer one over the other; however, all other runs used the 10 s average measurement model. In all eleven runs, SARSAT orbit-position error requirements were met despite the variety of parameter and starting values used.

The results with the tuned filter are contained in a twelfth run and are summarized in Table 1. Here, the estimator was started about 15 min prior to the first satellite pass with a position error of 13.584 km and a velocity error of 1376.5 cm/s (both of these errors are with respect to the definitive orbit data file, as are all errors quoted in this section). A diagonal a priori covariance of error matrix was adopted with optimistic values assumed for the variances of the orbit states. The range-rate data were biased by a margin of +1.0 km/s. Over the seven days of tracking data, there are a total of 39 passes. None of the errors during passes exceed 0.50 km in position and in only two of the passes do the errors exceed 0.35 km. In fact, no trend in the errors can be noted over the complete run and this property leads to the belief that the estimator has good long term performance.

Table 1 Performance of Kalman estimator using LANDSAT-III tracking data

		Selected error magnitudes		Selected position errors	
Day	Time, h:min	Position, km	Velocity, cm/s	Along track, km	Across track, km
1	(01:10)	(13.584)	(1376.5)	13.579)	(0.350)
	01:25[a]	0.345	19.4		
	03:07[a]	0.312	30.8		
	15:34[a]	0.403	61.8		
2	01:14[a]	0.302			
	01:23	0.240		0.258	0.052
	01:32	0.264	09.1		
	03:13[a]	0.226	26.8		
	14:00[a]	0.281	38.7		
	15:27[a]	0.440			
	15:36	0.276			
	15:45	0.274	41.4	0.142	0.234
3	01:37[a]	0.070	09.1		
	03:00[a]	0.202			
	03:09	0.221			
	03:18	0.228	26.6	0.092	0.208
	15:48[a]	0.117	33.7		
4	01:42[a]	0.077	10.6		
	03:23[a]	0.267	23.5		
	13:54[a]	0.124			
	14:03				
	14:12	0.140	22.1	0.066	0.123
	15:54[a]	0.064	31.7		
5	01:48[a]	0.129	12.8		
	14:00[a]	0.147			
	14:09	0.120			
	14:18	0.192	25.7	0.122	0.148
	16:00[a]	0.106	30.7		
6	01:36[a]	0.208			
	01:45	0.137			
	01:54	0.177	15.0	0.158	0.078
	14:23[a]	0.260	33.7		
	15:47[a]	0.273			
	15:56	0.162			
	16:05	0.170	31.9	0.158	0.062
7	01:42[a]	0.202			
	01:51	0.192			
	02:00	0.240	19.5	0.228	0.074
	15:53[a]	0.309			
	16:02	0.206			
	16:11	0.196	37.4	0.184	0.069

[a] Denotes samples from separate satellite passes.

Statistical Test of Externally-Supplied ODs

It is desirable to protect the estimator against accepting an OD that is grossly in error. An approach under evaluation is one in which the mean values (over one pass of data) of the correlation between consecutive innovations sequence members are compared, between the estimator operating with the newly received OD as an initial condition and the estimator operating with its current conditions.[9] Very large (i.e., highly correlated) values of this parameter are an indication of a nonwhite noise sequence; consequently, in the event that one of the compared values is very large with respect to the other it is probable that the estimator performance in that case is the poorer. This procedure has been observed to work adequately with simulated data which has pure white noise characteristics. The value of the parameter will be monitored during the testing in the advanced development Doppler processor (ADDP) and eventually during the demonstration phase to ascertain in situ its reliability as an OD-error filter.

Conclusions

The following conclusions may be drawn from this work.

Ephemeris Generation Method Using the Epoch-Time Estimator

1) The performance is strongly dependent upon the error characteristics of the ODs.

2) The estimator does not meet the requirements of 1.0 km in satellite orbit-position error with the population of ODs characteristic of TIROS-N.

3) OD rejection/acceptance criteria using the mean-squared measurement residual test appear to be adequate.

4) Selective rejection/acceptance of ODs does not fundamentally alter the performance of the estimator although maximum errors may be reduced slightly.

5) The method is capable of providing long term performance (several years) to an accuracy of 3 km for a system of similar design and characteristics.

Ephemeris Generation Method Using The Kalman Estimator

1) The performance has no significant dependence upon the error characteristics of the ODs.

2) The estimator is capable of providing satellite orbital position to within approximately 0.5 km.

3) OD rejection/acceptance criteria using the mean value of the correlation of consecutive innovations sequence members appear to be adequate.

4) Performance to date suggests the estimator has excellent potential in maintaining orbital position errors within SARSAT requirements for long term independent use.

Concluding Remarks

The method using the epoch-time estimator is comparatively simple conceptually and from a computation standpoint; however, it falls short of fulfilling the SARSAT system requirements of 1.0 km in satellite orbit-position error. This is principally a result of the dependence of its performance upon the error characteristics of the externally-supplied ODs. The error characteristics assumed in this work may or may not be a realistic description, but the existence of velocity errors up to 50 cm/s in the ODs makes it difficult to achieve SARSAT error requirements. In the runs described herein, none of the velocity errors exceed 30 cm/s. It seems likely that a velocity error of 10-20 cm/s would be the required maximum in an OD for use with the epoch-time estimator.

The method that utilizes an orbit-state Kalman estimator comfortably satisfies the SARSAT accuracy requirements and exhibits an insensitivity to errors in the orbit determination. The computer requirement at the LUT is substantially greater than with the other method but is not unreasonable for modern minicomputers or microprocessors. The method using the extended Kalman filter and the six parameter unified state model has been verified by processing range-rate data obtained from ETCA (Greenbelt, Md.) for LANDSAT-III. The method is able to determine orbital position to within 0.5 km. An orbit-state Kalman estimator-predictor method is presently baselined for the Canadian SARSAT LUT.

Acknowledgments

Grateful acknowledgment is made of the valuable contributions of H.I. El-Zorkany presently with Carleton University, and E.A. McPherson of SED Systems, several of whose reports are cited in the reference list. The encouragement of SARSAT project management, H.L. Werstiuk and R.J. Bibby in particular, was essential to the successful completion of the study.

References

[1] Trudel, B.J. and Winter, A.E., "Preliminary System Definition Document, Joint NASA/Canada Satellite-Aided Search and Rescue (SAR) Mission," NASA-GSFC, Greenbelt, Md., Department of Communications, CRC, Ottawa, Ontario, June 1, 1977.

[2] Werstiuk, H.L. and Winter, A.E., "The Search and Rescue (SARSAT) System Project," AGARD-CPP-238, *Operational Modelling of the Aerospace Propagation Environment,* April 1978, pp. 20-1, 20-12.

[3] Koch, D.W., "Error Analysis for Satellite-Aided Search and Rescue," NASA GSFC Rept. X-932-76-86, Aug. 1976.

[4] "U.S. SAR Mission Control Center Functions," Final Rept. for NASA, OAO Corporation, Beltsville, Md., Dec. 1977.

[5] Anderson, L.H., private communication, Operations Analysis Section, Operational Orbit Support Branch, NASA-GSFC, Greenbelt, Md., Jan. 1979.

[6] Schmid, P.E. and Lynn, J.J., "Satellite Doppler-Data Processing Using a Microcomputer," *IEEE Transactions on Geoscience Electronics,* Vol. GE-16, No. 4, Oct. 1978, pp. 340-349.

[7] McPherson, E.A. and Browne, H.J., "Orbit Determination and Prediction Mathematics," SED Systems Inc., Saskatoon, Sask., Doc. 91800-TR-101, March 1979.

[8] El-Zorkany, H.L., "SARSAT Orbit Parameter Estimator No. 1," Rept. for CRC, James D. Kendall Consultants Ltd., Mississauga, Ontario, May 1978.

[9] El-Zorkany, H.I., "Orbit Determination Acceptance Study," Rept. for CRC, James D. Kendall Consultants Ltd., Mississauga, Ontario, Feb. 1979.

[10] Gumbel, E.J., "Statistical Theory of Extreme Valves and Some Practical Applications," National Bureau of Standards, *Applied Mathematics Senes 33,* Feb. 12, 1954.

[11] Gumbel, E.J., "Probability Tables for the Analysis of Extreme-Value Data," National Bureau of Standards, *Applied Mathematics Series 22,* July 6, 1953.

[12] Jazwinski, A.H., *Stochastic Processes and Filtering Theory,* Academic Press, 1970, pp. 272-281.

[13] Gelb, A. (ed.), *Applied Optimal Estimation,* The M.I.T. Press, 1974, pp. 180-190.

[14] Altman, S.P. and Pistiner, J.S., "Application of State Space Transformation Theory to Orbit Determination and Prediction," AAS/AIAA Astrodynamics Specialists Conference, Jackson, Wyoming, Sept. 1968.

[15] SED Staff, "Comparison of Three Sets of Orbital Elements," SED Doc. 191800-TR-192, Jan. 1979.

[16] Salzberg, I.M., private communication, magnetic tape of 7 days of NASA raw tracking data for LANDSAT-III, Orbit Operations Section, Operational Orbit Support Branch, NASA-GSFC, Jan. 1979.

[17] Watkins, E.R., private communication, magnetic tape of 7 days of Definitive Orbit Data for LANDSAT-III, Operational Orbit Support Branch, NASA-GSFC, Nov. 1978.

[18] McPherson, E.A., "Orbit Determination Results from Range-Rate Data," SED Doc. 099500-TR-101, SED Systems Inc., Saskatoon, Sask., March 29, 1979.